

# Time-odd components in the mean field of rotating superdeformed nuclei

J.Dobaczewski<sup>(1,2)</sup> and J. Dudek<sup>(1)</sup>

<sup>(1)</sup>*Centre de Recherches Nucléaires, IN<sub>2</sub>P<sub>3</sub>-CNRS/Université Louis Pasteur  
F-67037 Strasbourg Cedex 2, France*

<sup>(2)</sup>*Institute of Theoretical Physics, Warsaw University  
ul. Hoża 69, PL-00681 Warsaw, Poland*

## Abstract

Rotation-induced time-odd components in the nuclear mean field are analyzed using the Hartree-Fock cranking approach with effective interactions SIII, SkM\*, and SkP. Identical dynamical moments  $\mathcal{J}^{(2)}$  are obtained for pairs of superdeformed bands  $^{151}\text{Tb}(2)$ – $^{152}\text{Dy}(1)$  and  $^{150}\text{Gd}(2)$ – $^{151}\text{Tb}(1)$ . The corresponding relative alignments strongly depend on which time-odd mean-field terms are taken into account in the Hartree-Fock equations.

PACS number(s): 21.60.-n, 21.60.Ev, 21.60.Jz

## I. INTRODUCTION

A description of ground and excited states in terms of a mean field is a well established approach in nuclear structure. Most of the nuclear phenomena can be considered as manifestations of the mean field properties, or the mean field can be used as a suitable framework and the first-order approximation. The mean field results from averaging the nucleon-nucleon interactions over states of individual nucleons. The averaging procedure, which must take into account the Fermi statistics of nucleons, can be formalized in terms of a variational approach, and leads to the well-known Hartree-Fock (HF) selfconsistent equations [1].

Dynamic or time-dependent phenomena can be described by a corresponding time-dependent HF method. The nuclear state is then represented by a one-body density matrix, which evolves in time according to the Hamilton equations, and represents a motion of a wave packet. Such an approach has been applied to genuinely time-dependent problems, like nuclear reactions, but it is in fact best suited to describe stationary collective states.

The nuclear rotation is an example of a collective motion for which linear combinations of stationary states of a given spin can be identified with a rotating wave packet. In this case, a transition from the time-dependent HF theory to a stationary problem can be achieved by introducing rotating intrinsic frame of reference. In this frame, the equations of motion are time-independent, however, the resulting density matrix is not invariant with respect to the time-reversal operator. As a consequence, the mean field obtained for such a density matrix also loses its time invariance, and acquires new terms which are odd with respect to the time reversal.

Properties of nuclear time-even mean fields are known rather well, because they are reflected in multiple static phenomena which can be studied experimentally [2]. On the other hand, very little is known about properties of the time-odd mean fields. Most studies were up to now carried out either within the adiabatic [3] or semiclassical approximations [4]. In particular, the adiabatic approximation to the nuclear translation, rotation, or quadrupole motion leads to the well-known Thouless-Valatin [5] corrections to the mass, moment of inertia, or to the vibrational mass parameters, respectively.

These corrections reflect the fact that a velocity-dependent mean field should be appropriately transformed to the intrinsic frame of reference [6] corresponding to a given collective mode. In fact, simple estimations and numerical calculations [7–9] show that the inertia obtained for effective forces without the effective-mass terms ( $m^*=m$ ) are very close to those for  $m^*<m$  when the Thouless-Valatin corrections are consistently included.

Fast nuclear rotation is a phenomenon in which the collective motion should be described beyond the adiabatic limit. Such a cranking model has been successfully used in explaining numerous high-spin effects in nuclei [10]. In this approach, the properties of the rotating mean field explicitly depend on the angular velocity. However, most studies performed up to now were done in terms of phenomenological mean fields, which are not selfconsistently depending on the rotating states, and, therefore, do not incorporate time-odd terms. Only in Ref. [11] an attempt has been made to include the effects of a zero-range interaction within the Nilsson single-particle mean field. Full selfconsistent cranking calculations [12–22] are still rather scarce, and no explicit analysis of the time-odd mean-field components is available.

On the other hand, the discovery of the superdeformation [23], and the resulting avalanche of very precise data on high-spin states, allow for an attempt to study these unknown aspects of the nuclear mean field. In particular, the phenomenon of identical bands (see Ref. [24] for a recent review) provides an extremely rich and puzzling information on properties of fast rotating states. In terms of the mean field approaches explicitly depending on the time-odd components, the calculated identical  $\gamma$ -ray transitions have been obtained in two cases only, namely, (i) the HF cranking calculations with Skyrme interaction gave yrast band of  $^{194}\text{Hg}$  identical to an excited band in  $^{194}\text{Pb}$  [14], and (ii) the identical bands in  $^{152}\text{Dy}$  and  $^{151}\text{Tb}$  (excited band) were obtained in the relativistic mean-field (RMF) theory [21]. In both studies, the authors invoked the time-odd components of the mean field as a crucial element of the obtained results.

In the present study we aim at a detailed analysis of these time-odd terms in the context of the identical bands phenomenon. We focus our attention on two classic and experimentally well studied pairs of identical bands, namely, on those in  $^{152}\text{Dy}$  and  $^{151}\text{Tb}$  (excited band), and in  $^{151}\text{Tb}$  and  $^{150}\text{Gd}$  (excited band). We perform our calculations in terms of the HF cranking method with the Skyrme interactions.

It was not in our intentions to give here a full account of the time-reversal breaking description that the selfconsistent HF cranking approach really offers and the experiment may test. Such a field of studies seems to emerge now in relation with the fast progress in the available experimental information. In particular, our choice of the illustrative material purposely minimizes rather than maximizes a possible magnitude of the time-odd effects. This is so, because we mainly discuss the role of the  $\pi[301]1/2$  Nilsson orbital known to interact only weakly via the Coriolis term in the hamiltonian.

In all standard approaches, such as the Woods-Saxon (WS), Nilsson, HF, or RMF cranking models, one signature member of this orbital is to a good approximation given by a straight line as a function of the angular velocity. This type of dependence can be opposed to dramatic changes of other aligning or interacting orbitals which are much more sensitive to the rotating field and hence to its time-odd components. On the other hand, the specific behavior of the discussed orbital induces a regular behavior of various observables, and has a great advantage in the fact that the level repulsion or level crossings do not disturb the comparisons of primary interest here.

In Section II we discuss the Skyrme interaction and energy density with a particular emphasis on the relations between the time-even and time-odd components of the mean field. The HF cranking calculations are presented in Section III, where several variants of the Skyrme functional are used and the influence of the time-odd terms on the rotational properties is analyzed, and conclusions are presented in Section IV.

## II. SKYRME ENERGY DENSITY

The Skyrme energy functional [25,26] is a three-dimensional integral

$$\mathcal{E} = \int d^3\mathbf{r} \mathcal{H}(\mathbf{r}) \quad (2.1)$$

of the energy density  $\mathcal{H}(\mathbf{r})$  which can be represented as a sum of the kinetic energy and of the potential-energy isoscalar and isovector terms

$$\mathcal{H}(\mathbf{r}) = \frac{\hbar^2}{2m}\tau_0 + \mathcal{H}_0(\mathbf{r}) + \mathcal{H}_1(\mathbf{r}), \quad (2.2)$$

where

$$\mathcal{H}_t(\mathbf{r}) = \mathcal{H}_t^{\text{even}}(\mathbf{r}) + \mathcal{H}_t^{\text{odd}}(\mathbf{r}), \quad (2.3)$$

with

$$\begin{aligned} \mathcal{H}_t^{\text{even}}(\mathbf{r}) &= C_t^\rho \rho_t^2 + C_t^{\Delta\rho} \rho_t \Delta\rho_t + C_t^\tau \rho_t \tau_t + C_t^J \overset{\leftrightarrow}{J}_t^2 + C_t^{\nabla J} \rho_t \nabla \cdot \mathbf{J}_t, \\ \mathcal{H}_t^{\text{odd}}(\mathbf{r}) &= C_t^s \mathbf{s}_t^2 + C_t^{\Delta s} \mathbf{s}_t \cdot \Delta \mathbf{s}_t + C_t^T \mathbf{s}_t \cdot \mathbf{T}_t + C_t^j \mathbf{j}_t^2 + C_t^{\nabla j} \mathbf{s}_t \cdot (\nabla \times \mathbf{j}_t), \end{aligned} \quad (2.4)$$

and the isospin index  $t$  can have values 0 or 1. Coupling constants  $C_t$  have superscripts corresponding to various density functions appearing in Eq. (2.4). All of these coupling constants can, in principle, depend on particle densities, see Refs. [27,28], but the most common choice [25,29] restricts the density dependence to the  $C_t^\rho$  and  $C_t^s$  terms. In Appendix A we give coupling constants  $C_t$  expressed through the traditional parameters of the Skyrme interaction.

Apart from the density-dependent coupling constants, the isoscalar energy density,  $\mathcal{H}_0(\mathbf{r})$ , depends on the isoscalar density functions and the isovector one,  $\mathcal{H}_1(\mathbf{r})$ , depends on the isovector density functions. For the particle densities,  $\rho_t$ , the isoscalar and isovector parts are defined in the usual way as a sum and a difference of the proton and neutron contributions, respectively,

$$\rho_0 = \rho_n + \rho_p \quad , \quad \rho_1 = \rho_n - \rho_p, \quad (2.5)$$

and analogous expressions are used to define other densities.

Altogether we have to consider six position-dependent density functions  $\rho$ ,  $\tau$ ,  $\mathbf{j}$ ,  $\mathbf{s}$ ,  $\mathbf{T}$  and  $\overset{\leftrightarrow}{J}$  with definitions given in Ref. [26]. Whenever the isospin indices are omitted, we understand that the symbols may refer either to the isoscalar ( $t=0$ ) or isovector ( $t=1$ ) parts.

In the energy densities (2.4) there appear two scalar time-even density functions,  $\rho$  and  $\tau$ , one vector time-odd,  $\mathbf{j}$ , and two pseudo-vector time-odd ones,  $\mathbf{s}$  and  $\mathbf{T}$ , and one pseudo-tensor time-even density function,  $\overset{\leftrightarrow}{J}$ . The vector time-even density  $\mathbf{J}$  which appears in Eq. (2.4) is given by the antisymmetric part of the pseudo-tensor density, i.e.,  $J_\lambda = \sum_{\mu\nu} \epsilon_{\lambda\mu\nu} J_{\mu\nu}$ , and is not an independent quantity. Terms in  $\mathcal{H}_t^{\text{even}}(\mathbf{r})$  and  $\mathcal{H}_t^{\text{odd}}(\mathbf{r})$  are bilinear in time-even and time-odd densities, respectively. Therefore, we denote them by the superscripts “even” and “odd”. This notation is only used to indicate the dependence on two different classes of densities. It should not be confused with the fact that both  $\mathcal{H}_t^{\text{even}}(\mathbf{r})$  and  $\mathcal{H}_t^{\text{odd}}(\mathbf{r})$  are of course *even* with respect to the time reversal. To every term in  $\mathcal{H}_t^{\text{even}}(\mathbf{r})$  there corresponds an analogous term in  $\mathcal{H}_t^{\text{odd}}(\mathbf{r})$ , as seen in Eq. (2.4).

## A. Mean fields

By varying the energy density (2.4) with respect to the six density functions  $\rho$ ,  $\tau$ ,  $\mathbf{j}$ ,  $\mathbf{s}$ ,  $\mathbf{T}$  and  $\overset{\leftrightarrow}{J}$  one obtains the mean fields. Details of calculations are presented in Ref. [26]. Here

we only repeat the final results conforming to the notation introduced above. Time-even and time-odd mean fields are obtained by a variation of  $\mathcal{H}_t^{\text{even}}(\mathbf{r})$  and  $\mathcal{H}_t^{\text{odd}}(\mathbf{r})$ , respectively, and they read

$$\begin{aligned}\Gamma_t^{\text{even}} &= -\nabla \cdot M_t(\mathbf{r})\nabla + U_t(\mathbf{r}) + \frac{1}{2i}(\overleftrightarrow{\nabla}\sigma \cdot \overleftrightarrow{B}_t(\mathbf{r}) + \overleftrightarrow{B}_t(\mathbf{r}) \cdot \overleftrightarrow{\nabla}\sigma), \\ \Gamma_t^{\text{odd}} &= -\nabla \cdot (\boldsymbol{\sigma} \cdot \mathbf{C}_t(\mathbf{r}))\nabla + \boldsymbol{\sigma} \cdot \boldsymbol{\Sigma}_t(\mathbf{r}) + \frac{1}{2i}(\nabla \cdot \mathbf{I}_t(\mathbf{r}) + \mathbf{I}_t(\mathbf{r}) \cdot \nabla).\end{aligned}\quad (2.6)$$

These fields are given by the six potential functions  $U$ ,  $M$ ,  $\mathbf{I}$ ,  $\boldsymbol{\Sigma}$ ,  $\mathbf{C}$  and  $\overleftrightarrow{B}$  which have tensor transformation properties respectively identical to the six density functions on which they depend through the following formulae

$$U_t = 2C_t^\rho \rho_t + 2C_t^{\Delta\rho} \Delta\rho_t + C_t^\tau \tau_t + C_t^{\nabla J} \nabla \cdot \mathbf{J}_t, \quad (2.7a)$$

$$\boldsymbol{\Sigma}_t = 2C_t^s \mathbf{s}_t + 2C_t^{\Delta s} \Delta\mathbf{s}_t + C_t^T \mathbf{T}_t + C_t^{\nabla j} \nabla \times \mathbf{j}_t, \quad (2.7b)$$

$$M_t = C_t^\tau \rho_t, \quad (2.7c)$$

$$\mathbf{C}_t = C_t^T \mathbf{s}_t, \quad (2.7d)$$

$$\overleftrightarrow{B}_t = 2C_t^{J\overleftrightarrow{j}} \mathbf{j}_t - C_t^{\nabla J} \overleftrightarrow{\nabla} \rho_t, \quad (2.7e)$$

$$\mathbf{I}_t = 2C_t^j \mathbf{j}_t + C_t^{\nabla j} \nabla \times \mathbf{s}_t, \quad (2.7f)$$

The tensor gradient operators in Eqs. (2.6) and (2.7e) are defined [26] as  $(\overleftrightarrow{\nabla}\sigma)_{\mu\nu} = \nabla_\mu \sigma_\nu$  and  $\nabla_{\mu\nu} = \sum_\lambda \epsilon_{\mu\nu\lambda} \nabla_\lambda$ .

Due to the density dependence of the coupling constants  $C_t^\rho$  and  $C_t^s$  one has to add to the isoscalar potential energy  $U_0$  the rearrangement terms [1] resulting from the variation of these coupling constants with respect to the isoscalar particle density, i.e.,

$$U'_0 = \sum_t \left( \frac{\partial C_t^\rho}{\partial \rho_0} \rho_t^2 + \frac{\partial C_t^s}{\partial \rho_0} \mathbf{s}_t^2 \right). \quad (2.8)$$

These terms introduce an explicit dependence of the complete time-even isoscalar potential  $U_0 + U'_0$  on the isovector density  $\rho_1$  and on the time-odd densities  $\mathbf{s}_t^2$ . Similar terms have to be also consistently taken into account whenever some other coupling constants are assumed to be density dependent.

Finally, the neutron and proton hamiltonians,  $h_n$  and  $h_p$ , are obtained by combining the kinetic energy with the isoscalar and isovector mean fields:

$$h_n = -\frac{\hbar^2}{2m} \Delta + \Gamma_0^{\text{even}} + \Gamma_0^{\text{odd}} + \Gamma_1^{\text{even}} + \Gamma_1^{\text{odd}}, \quad (2.9)$$

$$h_p = -\frac{\hbar^2}{2m} \Delta + \Gamma_0^{\text{even}} + \Gamma_0^{\text{odd}} - \Gamma_1^{\text{even}} - \Gamma_1^{\text{odd}}.$$

We are now in a position to discuss different time-odd terms in the mean fields. It is clear that the time-odd mean fields,  $\Gamma_t^{\text{odd}}$ , in Eq. (2.6) directly result from the ‘‘odd’’ part,  $\mathcal{H}_t^{\text{odd}}(\mathbf{r})$ , of the energy density in (2.4), and depend on 10 time-odd coupling constants  $C_t^s$ ,  $C_t^{\Delta s}$ ,  $C_t^T$ ,  $C_t^j$ , and  $C_t^{\nabla j}$  for  $t=0$  and  $t=1$ . Similarly, the time-even mean fields depend on 10 time-even coupling constants  $C_t^\rho$ ,  $C_t^{\Delta\rho}$ ,  $C_t^\tau$ ,  $C_t^J$ , and  $C_t^{\nabla J}$ . For the Skyrme interaction, the time-odd

coupling constants are linear combinations of the time-even ones (see Appendix A), and therefore the time-odd mean fields are uniquely determined from the time-even mean fields. Since the time-even fields are tested against numerous experimental observations which have a static character, they are much better known than the time-odd ones. In fact, the Skyrme force parameters have been in the past almost uniquely fitted to the static properties only. A description of dynamic properties which do depend on the time-odd fields does not therefore (for the Skyrme force) require new parameters to be introduced and fitted.

On the other hand, one sometimes adopts a different point of view by considering the energy density to be a more fundamental construction than the Skyrme interaction itself [30]. In such a case, all 20 coupling constants of Eq. (2.4) should be treated and adjusted independently. However, in the next Section we show that some relations between time-odd and time-even coupling constants have an origin in the local gauge invariance of the energy density.

### B. Local gauge invariance

As noted in Ref. [26], in the energy density derived from the Skyrme interaction the kinetic density  $\tau$  and the current density  $\mathbf{j}$  appear in the characteristic combination of  $\rho_t\tau_t - \mathbf{j}_t^2$ . The same is true for two other pairs of densities appearing together in the combinations  $\mathbf{s}_t \cdot \mathbf{T}_t - \overleftrightarrow{J}_t^2$  and  $(\rho_t \nabla \cdot \mathbf{J}_t + \mathbf{s}_t \cdot (\nabla \times \mathbf{j}_t))$ . This gives the following relations between three pairs of time-even and time-odd coupling constants

$$C_t^j = -C_t^\tau, \quad (2.10a)$$

$$C_t^J = -C_t^T, \quad (2.10b)$$

$$C_t^{\nabla j} = +C_t^{\nabla J}. \quad (2.10c)$$

The Skyrme functional has now the form

$$\begin{aligned} \mathcal{H}_t(\mathbf{r}) = & C_t^\rho \rho_t^2 + C_t^s \mathbf{s}_t^2 + C_t^{\Delta\rho} \rho_t \Delta\rho_t + C_t^{\Delta s} \mathbf{s}_t \cdot \Delta\mathbf{s}_t \\ & + C_t^\tau (\rho_t \tau_t - \mathbf{j}_t^2) + C_t^T (\mathbf{s}_t \cdot \mathbf{T}_t - \overleftrightarrow{J}_t^2) \\ & + C_t^{\nabla J} (\rho_t \nabla \cdot \mathbf{J}_t + \mathbf{s}_t \cdot (\nabla \times \mathbf{j}_t)). \end{aligned} \quad (2.11)$$

In Ref. [26] this structure has been interpreted as a result of the Galilean invariance of the Skyrme interaction. However, it has a deeper origin in the fact that the Skyrme force is locally gauge invariant. In order to illustrate the role of the locally gauge invariant, velocity dependent interactions let us consider an arbitrary finite-range and non-local, but velocity independent interaction given by

$$\hat{V} = V(\mathbf{r}'_1, \mathbf{r}'_2; \mathbf{r}_1, \mathbf{r}_2). \quad (2.12)$$

To simplify the notation we disregard for a moment the spin and isospin variables.  $\hat{V}$  describes an interaction process where the particles 1 and 2 are located at  $\mathbf{r}_1$  and  $\mathbf{r}_2$  before the interaction, and at  $\mathbf{r}'_1$  and  $\mathbf{r}'_2$  after the interaction. When the system of particles is described by a one-body density matrix  $\rho(\mathbf{r}, \mathbf{r}')$ , its HF interaction energy reads

$$\mathcal{E}^{\text{int}} = \int d\mathbf{r}'_1 d\mathbf{r}'_2 d\mathbf{r}_1 d\mathbf{r}_2 V(\mathbf{r}'_1, \mathbf{r}'_2; \mathbf{r}_1, \mathbf{r}_2) \times (\rho(\mathbf{r}_1, \mathbf{r}'_1)\rho(\mathbf{r}_2, \mathbf{r}'_2) - \rho(\mathbf{r}_2, \mathbf{r}'_1)\rho(\mathbf{r}_1, \mathbf{r}'_2)). \quad (2.13)$$

For a local gauge transformation of the many-body HF wave function  $|\Psi\rangle$ ,

$$|\Psi'\rangle = \exp\left\{i\sum_{j=1}^A \phi(\mathbf{r}_j)\right\} |\Psi\rangle, \quad (2.14)$$

where  $\phi(\mathbf{r})$  is an arbitrary real function of the position  $\mathbf{r}$ , one obtains the following gauge-transformed one-body density matrix

$$\rho'(\mathbf{r}, \mathbf{r}') = \exp\left\{i(\phi(\mathbf{r}) - \phi(\mathbf{r}'))\right\} \rho(\mathbf{r}, \mathbf{r}'). \quad (2.15)$$

The general interaction energy (2.13) is not invariant with respect to such a transformation. However, when the interaction is local [1],

$$V(\mathbf{r}'_1, \mathbf{r}'_2; \mathbf{r}_1, \mathbf{r}_2) = \delta(\mathbf{r}'_1 - \mathbf{r}_1)\delta(\mathbf{r}'_2 - \mathbf{r}_2)V(\mathbf{r}_1, \mathbf{r}_2), \quad (2.16)$$

the corresponding interaction energy,

$$\mathcal{E}^{\text{int}} = \int d\mathbf{r}_1 d\mathbf{r}_2 V(\mathbf{r}_1, \mathbf{r}_2) \times (\rho(\mathbf{r}_1)\rho(\mathbf{r}_2) - \rho(\mathbf{r}_2, \mathbf{r}_1)\rho(\mathbf{r}_1, \mathbf{r}_2)), \quad (2.17)$$

becomes invariant with respect to the local gauge. The direct term is invariant because it depends only on the gauge-invariant local densities, which are denoted by the single argument, i.e.,  $\rho(\mathbf{r}) \equiv \rho(\mathbf{r}, \mathbf{r})$ . On the other hand, in the exchange term the gauge factors coming from two density matrices cancel one another.

When the density functions defining the Skyrme energy functional (2.4) are calculated for the gauge-transformed density matrix (2.15) one obtains the following relations:

$$\rho' = \rho \quad (2.18a)$$

$$\tau' = \tau + 2\mathbf{j} \cdot \nabla\phi + \rho(\nabla\phi)^2, \quad (2.18b)$$

$$s'_k = s_k, \quad (2.18c)$$

$$j'_k = j_k + \rho\nabla_k\phi, \quad (2.18d)$$

$$T'_k = T_k + 2\sum_l J_{kl}\nabla_l\phi + s_k(\nabla\phi)^2, \quad (2.18e)$$

$$J'_{kl} = J_{kl} + s_l\nabla_k\phi, \quad (2.18f)$$

and the three characteristic combinations of density functions, which appear in the energy density of Eq. (2.11), are then explicitly gauge invariant. Transformation properties of  $\tau$  and  $\mathbf{j}$  allow to interpret  $\nabla\phi$  as a velocity field,

$$\mathbf{v} = \frac{\hbar}{m}\nabla\phi, \quad (2.19)$$

which shows that the flow of matter obtained through the gauge transformation is irrotational,  $\nabla \times \mathbf{v} = 0$ .

The local gauge invariance of the Skyrme interaction reflects the fact that its velocity dependence has been introduced only to simulate the finite range effects of the effective interaction. In this way the Skyrme interaction conserves the local gauge invariance of a velocity-independent finite-range local interaction, such as the Gogny force [1], for example.

### 1. Translational motion

The Galilean invariance is a special case of the local gauge invariance, for which the phase in Eq. (2.14) is given by

$$\phi(\mathbf{r}) = \frac{\mathbf{p} \cdot \mathbf{r}}{\hbar}, \quad (2.20)$$

where  $\mathbf{p}$  is a constant linear momentum of the boost transformation. Since the interaction energy does not depend on  $\mathbf{p}$ , the total energy (2.1) is only modified through the kinetic energy [the first term in Eq. (2.2)]. Using the transformation property of  $\tau$ , Eq. (2.18b), we have the energy increase under the boost transformation,

$$\Delta\mathcal{E}^{\text{boost}} = \frac{\mathbf{p}^2}{2m}A, \quad (2.21)$$

equal to the translational energy of the boosted system. This result holds for an initially stationary solution (i.e., for vanishing currents,  $\mathbf{j}=0$ ), however, due to the transformation property of  $\mathbf{j}$ , Eq. (2.18d), the boost transformations can be added to one another by adding the corresponding momenta  $\mathbf{p}$ . For the boost transformation, one obtains the obvious velocity field (2.19), i.e.,

$$\mathbf{v}^{\text{boost}} = \frac{\mathbf{p}}{m}. \quad (2.22)$$

### 2. Rotational motion

Since the velocity field (2.19) obtained through a gauge transformation is irrotational, it cannot correctly describe physical rotations of nuclei. This is so, because the nuclei basically rotate as rigid bodies (at least in the independent-particle approximation [6]), and the velocity field of a rigid-body rotation,  $\mathbf{v}^{\text{rigid}} = \boldsymbol{\omega} \times \mathbf{r}$ , has a non-zero curl,  $\nabla \times \mathbf{v}^{\text{rigid}} = 2\boldsymbol{\omega}$ , i.e., is not irrotational. Of course, interactions and nucleon-nucleon correlations (pairing) introduce an irrotational component in the velocity field (moment of inertia decreases below the rigid-body value), but this field is never entirely irrotational.

In an analogy to the boost transformation, one may try to induce the rotation of a many-fermion system by adding for all particles a constant value,  $j_x$ , to their projections of the angular momentum on a fixed (say  $x$ ) axis. Such a procedure can be realized in terms of the twirl transformation given by the gauge function

$$\phi(\mathbf{r}) = \frac{j_x \arctan(z/y)}{\hbar}. \quad (2.23)$$

Its velocity field has the form

$$\mathbf{v}^{\text{twirl}} = \frac{j_x}{m\omega\eta(y,z)^2} \boldsymbol{\omega} \times \mathbf{r}, \quad (2.24)$$

where  $\boldsymbol{\omega}$  is the vector of angular velocity oriented along the  $x$  axis, and  $\eta(y,z)$  is the distance to this axis. One can see that the velocity field (2.24) is singular at the rotation axis. The

energy increase resulting from the kinetic energy density (2.18b) is then infinite for any arbitrarily small  $j_x$ . The irrotational velocity field (2.24) is of course very much different from the rigid-rotation velocity field,  $\mathbf{v}^{\text{rigid}}$ , even though both contain the same factor  $\boldsymbol{\omega} \times \mathbf{r}$ .

This illustrative example shows that the nuclear rotation cannot be realized by democratically distributing the angular momentum among all particles. In the cranking approximation, at a given value of the angular velocity some particles receive larger contributions (aligning states) and some smaller contributions (high- $K$  states). A precise distribution cannot be found without actually solving the quantal cranking equations. This example also shows that the gauge-invariant interaction must contribute to the rotational energy, contrary to what happens in the case of the translational motion.

### III. HARTREE-FOCK CRANKING CALCULATIONS

In the present study we have performed the Hartree-Fock (HF) calculations of superdeformed rotational bands using the Skyrme effective interactions. The calculations have been done using the numerical code HFODD which employs a three-dimensional cartesian deformed harmonic oscillator (HO) basis to describe the single-particle wave functions. The details concerning the HFODD code will be presented elsewhere [31]; here we only give a few of its basic parameters pertaining to the present application.

The calculations have been performed using a fixed basis given by the HO frequencies  $\hbar\omega_{\perp}=11.200$  and  $\hbar\omega_{\parallel}=6.246$  MeV in the directions perpendicular and parallel to the symmetry axis, respectively. These values have been obtained by standard prescriptions developed for diagonalizing the deformed WS hamiltonian [32,33] in the HO basis, and correspond to the WS potential with deformations  $\beta_2=0.61$  and  $\beta_4=0.10$ . The basis has been restricted to a fixed number,  $M$ , of basis states having the lowest single-particle HO energies  $\epsilon_{HO}=(n_x+n_y+1)\hbar\omega_{\perp}+(n_z+\frac{1}{2})\hbar\omega_{\parallel}$ . The actual calculations have been performed with  $M=306$ . This corresponds to the maximal numbers of oscillator quanta equal to 8 and 15 in the perpendicular and parallel directions, respectively.

The stability of results with respect to increasing the size of the HO basis has been tested by performing calculations with  $M=604$ , which introduces basis states up to 11 and 20 quanta in these two directions. It has been found that the rotational characteristics of the studied nuclei are almost independent of such an increase. For example, numerical inaccuracies in the dynamical moment  $\mathcal{J}^{(2)}$  and in the total angular momentum  $I$  can be estimated to be smaller than  $0.2\hbar^2\text{MeV}^{-1}$  and  $0.1\hbar$ , respectively. Inaccuracies of relative values between different angular frequencies  $\omega$ , or between different nuclei, are smaller than these estimates, because the numerical errors then cancel out.

In the present study we aim at investigating the role of different time-odd terms in the selfconsistent mean fields (2.6) obtained for rotating superdeformed nuclei. As discussed in Section II, this can be done by considering different values of 10 time-odd coupling constants appearing in the Skyrme energy density, Eq. (2.4). For every given set of values of coupling constants we perform full selfconsistent calculations within the HF cranking method. In the present study, pairing correlations are not taken into account. Below we separately discuss three cases corresponding to (i) the complete Skyrme functional, (ii) the Skyrme functional with certain time-odd terms omitted, but with the gauge invariance preserved, and (iii) with the gauge invariance violated.

As discussed in Section II B, the energy functionals corresponding to the standard Skyrme interactions preserve the local gauge invariance. The 20 coupling constants appearing in Eq. (2.4) are then restricted by 6 conditions (2.10a)-(2.10c), which leads to the energy density of Eq. (2.11). In Table I, the remaining 14 coupling constants are listed for the SIII [29], SkM\* [34], and SkP [35] Skyrme interactions. The values of the density-dependent coupling constants  $C_t^\rho$  and  $C_t^s$  are given for the vacuum ( $\rho=0$ ) and for the nuclear-matter saturation density ( $\rho=\rho_{\text{nm}}$ ) characterizing a given force.

The time-even coupling constants corresponding to the SIII, SkM\*, and SkP interactions are rather similar. The main difference consists in different values of the isoscalar-effective-mass coupling constant  $C_0^\tau$  which is equal to 0 for SkP (effective mass  $m^*/m=1$ ), and  $44.4 \text{ MeV}\cdot\text{fm}^5$  and  $34.7 \text{ MeV}\cdot\text{fm}^5$  for SIII and SkM\*, respectively (effective masses  $m^*/m=0.76$  and  $0.79$ ). Apart from that, the absolute values of the  $C_t^\rho$  coupling constants are larger for SkP than for SIII and SkM\*, which gives better symmetry-energy properties [36] within the SkP parametrization as compared to the other two forces. On the other hand, the SkM\* parameters have been adjusted so as to properly describe the surface energy at large deformation, and therefore this interaction was successfully applied in numerous studies of superdeformation.

Values of the time-odd coupling constants corresponding to the three Skyrme interactions, Table I, differ much more than those of the time-even ones. This illustrates uncertainties in determining the time-odd components of the mean field. The differences partly result from the fact that SkP has been adjusted to give attractive matrix elements in the pairing channel, while those given by SIII and SkM\* are repulsive. One should bear in mind, however, that for the Skyrme interaction the time-odd coupling constants are unique functions of the time-even ones (see Appendix A) and, in principle, one has no freedom for an independent readjustment. Such a readjustment is possible only if we consider the HF theory based directly on the energy density functional and not on the Skyrme interaction.

In the previous applications of the Skyrme force to nuclear rotation [12–15], in the energy density (2.11) the terms  $C_t^{\Delta s}$  and  $C_t^T$  have been neglected in order to facilitate the calculations. The first of these terms gives purely time-odd contribution to the mean field, while the second one gives both time-even and time-odd contributions, because the gauge invariance implies that  $C_t^T=C_t^J$ , Eq. (2.10b). In fact, the term  $C_t^J$  has also been usually neglected in most Skyrme parametrizations applied to problems where the time-reversal symmetry is concerned, cf. Ref. [29]. Since the HFODD code is organized in a different way, omitting some terms would not provide any serious simplifications, and the code may in fact handle the complete Skyrme functional. This gives us a possibility to test the importance of different terms for the rotational properties of nuclei.

There exist several high-spin observables which, when calculated from the HF solutions (wave functions) behave differently depending on whether various time-odd terms are included or not. This offers, in principle, a possibility of both better readjustment of the interaction coupling constants and better understanding of the underlying mechanisms. Some of the physical quantities, as e.g. alignments and  $\mathcal{J}^{(2)}$ -moments of intruder orbitals, are well recognized as responding strongly to the Coriolis and centrifugal interaction effects. The same quantities are expected to respond relatively strongly to the time-odd terms in the mean-field hamiltonian. Similarly, various families of orbitals having large high- $j$  components are systematically responsible for such precisely measurable effects as band-crossings

(back- or up-bending effects) and related phenomena.

In this study we would like to illustrate the effects of the time-odd terms on yet another seemingly more subtle mechanism related to identical bands, leaving the aforementioned analysis of intruder orbitals for a later investigation.

In the following Sections we present results of the HF cranking calculations for the yrast superdeformed bands in dysprosium,  $^{152}\text{Dy}(1)$ , and terbium,  $^{151}\text{Tb}(1)$ , and for the first excited bands in the corresponding isotones,  $^{151}\text{Tb}(2)$  and  $^{150}\text{Gd}(2)$ . According to the standard notation, the numbers in parentheses refer to numbers attributed in experimental studies in connection with relative intensities of gamma transitions. The experimental data are taken from Refs. [37–39] where the most recent and precise results are given.

The pairs of superdeformed bands,  $^{151}\text{Tb}(2)$ – $^{152}\text{Dy}(1)$  and  $^{150}\text{Gd}(2)$ – $^{151}\text{Tb}(1)$ , are identical with a very high precision [40]. For each pair, the  $\gamma$ -ray transition energies  $E_\gamma$  are identical up to 2 keV. The identity of the bands can be characterized in two ways, (i) by their relative alignments, and (ii) by their relative dynamical moments. The relative alignment  $\delta I$  is defined as a difference of spins in two bands at fixed angular velocity  $\omega$ . Similarly, the relative dynamical moment  $\delta\mathcal{J}^{(2)}$  is the difference of  $\mathcal{J}^{(2)}$  at the same value of  $\omega$ . In calculations, the latter is a derivative of the former with respect to the angular velocity.

In the present study we have fixed the yrast proton configurations of  $^{152}\text{Dy}$  and  $^{151}\text{Tb}$  to (16,16,17,17) and (15,16,17,17), respectively. The numbers in parentheses denote the numbers of lowest states occupied in the parity-signature blocks ordered as  $(++,+,-,-+,-,-)$ , where the signs denote the parity quantum number and the sign of the (imaginary) signature [6] quantum number,  $r=\pm i$ . One sometimes uses a notation based on the signature index  $\alpha$  which equals to  $-1/2(+1/2)$  for  $r=+i(-i)$ . For all bands considered in the present study, the neutron configurations are fixed at (22,22,21,21). The yrast configuration in  $^{151}\text{Tb}$  corresponds to a hole in the 16-th orbital in the  $++$  block,  $16^{++}$ , which in the standard notation is described as the  $\pi[651]3/2$  ( $r=+i$ ) or  $\pi 6_4$  Nilsson intruder orbital.

Since in the experiment the angular velocity is associated with half of the transition energy  $E_\gamma$ , and the above pairs of bands have identical transition energies, the relative alignments must be close to a half-integer value. This is simply a consequence of the fact that the spins in the odd and even nuclei are half-integer and integer, respectively. Departures from half-integer relative alignments can only be caused by differences in the  $\gamma$ -ray transition energies, which are very small for the two pairs of bands studied here. Since the values of spins have not yet been measured, the relative alignments are known up to an additive integer value and a theoretical input is necessary if one wishes to put forward one value or another.

Already at a very early stage of the identical band studies, it has been suggested [41] that the first excited bands  $^{151}\text{Tb}(2)$  and  $^{150}\text{Gd}(2)$  correspond to the  $\pi[301]1/2$  ( $r=+i$ ) holes (signature index  $\alpha=-1/2$ ) in the yrast states of the respective cores (see also Ref. [42]). In the present study we have followed this interpretation and we have constructed the excited bands by creating a hole in the 17-th orbital of the  $-+$  block,  $17^{-+}$ .

In all the WS and HF cranking calculations, the single-particle routhian  $\pi[301]1/2$  ( $r=+i$ ) increases with rotational frequency with a constant slope of about  $+0.5\hbar$ , i.e., it has the single-particle alignment (the average value of the projection of angular momentum on the rotation axis) close to  $-0.5\hbar$ . Therefore, a hole created in this orbital must lead to relative alignment of about  $+0.5\hbar$ . In this paper we adopt this half-integer value for fixing the

unknown integer additive constant,  $\delta I_0 = +0.5 \hbar$ , required to extract relative alignment from experimental data. Within this choice, the experimental average relative alignment for the  $^{151}\text{Tb}(2)$ – $^{152}\text{Dy}(1)$  pair of bands equals to  $+0.564(18) \hbar$ . The error given here is the average error resulting from experimental errors of transition energies. The experimental relative alignment for the  $^{150}\text{Gd}(2)$ – $^{151}\text{Tb}(1)$  pair increases slightly with the angular velocity and has the average value of  $+0.479(14) \hbar$ . In fact, experimentally, only the average departures from the half-integer constant  $\delta I_0$ ,  $\langle \delta I \rangle = \delta I_0 + 0.064(18) \hbar$  and  $\langle \delta I \rangle = \delta I_0 - 0.021(14) \hbar$ , are established.

### A. Complete Skyrme functionals

In Figs. 1 and 2 we show results of calculations for the  $^{151}\text{Tb}(2)$ – $^{152}\text{Dy}(1)$  and  $^{150}\text{Gd}(2)$ – $^{151}\text{Tb}(1)$  pairs of bands, respectively. The complete Skyrme energy-density functionals of the SIII, SkM\*, and SkP forces have been used. Parts (a) of these Figures (bottom) present the dynamical moments  $\mathcal{J}^{(2)}$  as functions of the angular velocity  $\omega$ .

#### 1. Dynamical moments $\mathcal{J}^{(2)}$

For  $^{152}\text{Dy}(1)$ , Fig. 1, all forces overestimate the experimental values of  $\mathcal{J}^{(2)}$  by about 5-10%. All three forces give very similar results, within  $2 \hbar^2 \text{MeV}^{-1}$ . A similarity of results obtained for different forces is also visible in Table II, where we give the values of proton quadrupole moments calculated at  $\omega = 0.5 \text{ MeV}/\hbar$ . The SIII interaction gives values larger by only 0.3–0.4 b as compared to those given by SkM\*, while the SkP force leads to intermediate results. A similarity of results for changes of proton quadrupole moments induced by creating holes in proton orbitals is even more pronounced. A polarization by the  $\pi[301]1/2$  ( $r=+i$ ) hole gives, for different forces, the changes between 0.12 b and 0.15 b. That induced by the  $\pi[651]3/2$  ( $r=+i$ ) hole gives values between  $-0.94$  b and  $-1.05$  b. The HF proton quadrupole moment of  $^{152}\text{Dy}(1)$  agrees very well with the result obtained within the Nilsson single-particle potential [42].

In Fig. 2(a) we show the dynamical moments  $\mathcal{J}^{(2)}$  calculated for the  $^{151}\text{Tb}(1)$  band. Due to the hole in the  $\pi[651]3/2$  ( $r=+i$ ) intruder orbital,  $\mathcal{J}^{(2)}$  decreases here with  $\omega$  much faster than that of the  $^{152}\text{Dy}(1)$  band. However, at  $\omega \simeq 0.45 \text{ MeV}/\hbar$  one obtains values of  $\mathcal{J}^{(2)} \simeq 94 \hbar^2 \text{MeV}^{-1}$  which are almost identical for all the forces and for both bands. This contradicts simple perturbative estimates. Indeed, a hole in the  $^{152}\text{Dy}(1)$  core should in principle cause a decrease of the moment of inertia due to the smaller mass and deformation of  $^{151}\text{Tb}(1)$ , and also due to the fact that the  $\pi[651]3/2$  ( $r=+i$ ) routhian has negative second derivative with respect to  $\omega$  and, therefore, the hole in this orbital should bring negative perturbative contribution to  $\mathcal{J}^{(2)}$ . Nevertheless, at  $\omega \simeq 0.45 \text{ MeV}/\hbar$  the  $\mathcal{J}^{(2)}$  values calculated for  $^{152}\text{Dy}(1)$  and  $^{151}\text{Tb}(1)$  are the same. This illustrates the fact that the polarization effects obtained by selfconsistent calculations do not necessarily follow perturbative estimates.

In  $^{151}\text{Tb}(1)$ , the SIII and SkM\* forces give a better agreement with data than SkP. This can be attributed to a different effective masses,  $m^*/m=1$  for SkP and 0.76–0.79 for SIII and SkM\*, which leads to different time-odd components in the mean field (see the next Section).

Then, the interaction between the intruder orbital  $\pi[651]3/2$  ( $r=+i$ ) and the time-odd mean field is modified, and gives a more significant departure from experiment.

### 2. Relative dynamical moments $\delta\mathcal{J}^{(2)}$

In parts (b) of Figs. 1 and 2 we present the relative dynamical moments  $\delta\mathcal{J}^{(2)}$  calculated for the pairs of bands  $^{151}\text{Tb}(2)\text{--}^{152}\text{Dy}(1)$  and  $^{150}\text{Gd}(2)\text{--}^{151}\text{Tb}(1)$ , respectively. One should note that the scale in (b) is enlarged five times with respect to that in (a). At  $\omega > 0.3 \text{ MeV}/\hbar$ , both pairs of bands have dynamical moments identical up to about  $1 \hbar^2 \text{ MeV}^{-1}$ , with lighter isotones having slightly larger values. In the scale of (a) this would lead to curves identical up to the size of the data marks.

This result confirms the observation [14] that the identity of dynamical moments can in fact be obtained in self-consistent theories, and does not necessarily follow semiclassical [43] or perturbative estimates. The experimental values of  $\delta\mathcal{J}^{(2)}$  are not shown in parts (b), because they would be scattered between  $\pm 1.5 \hbar^2 \text{ MeV}^{-1}$  with errors between 1 and  $2.5 \hbar^2 \text{ MeV}^{-1}$ , i.e., in the scale of (b) they would cover the whole presented region of  $\delta\mathcal{J}^{(2)}$ .

### 3. Relative alignments $\delta I$

The calculated relative alignments  $\delta I$ , shown in parts (c) of Figs. 1 and 2, do not reproduce experimental results with a sufficient precision. For the  $^{151}\text{Tb}(2)\text{--}^{152}\text{Dy}(1)$  pair [Fig. 1(c)], in the region of  $\omega$  where the data are available, one obtains a gradual increase of  $\delta I$  by almost  $0.5 \hbar$ . For the SIII and SkP forces the value obtained at  $\omega = 0.3 \text{ MeV}/\hbar$  is correct, but for SkM\* the whole curve is additionally shifted up by about  $0.5 \hbar$ . For the  $^{150}\text{Gd}(2)\text{--}^{151}\text{Tb}(1)$  calculations this increase becomes smaller (SIII and SkP) and similar to the small increase seen in the experimental data. However, the values of  $\delta I$  are still slightly (SIII and SkP) or significantly (SkM\*) too large.

Values of relative alignments can be translated into the differences  $\delta E_\gamma$  of  $\gamma$ -transition energies between the two bands. Using a linear local expansion of spin as function of the angular frequency we obtain that

$$\delta E_\gamma \simeq 2\hbar\delta\omega \simeq 2\hbar \frac{\delta I - \delta I_0}{\mathcal{J}^{(2)}}, \quad (3.1)$$

where  $\delta\omega$  is the difference of frequencies at spins of physical states in two nuclei. Hence the departures of calculated relative alignments  $\delta I$  from  $\delta I_0 = 0.5 \hbar$  correspond to the values of  $\delta E_\gamma$  between 0 and 10 keV, while the measured values are between 0 and 2 keV. In the following two sections we present calculations obtained with modified Skyrme functionals. In this way we try to analyze the influence of the time-odd terms on the relative alignments discussed here.

## B. Modified gauge-invariant Skyrme functionals

As discussed above, the gauge-invariance conditions (2.10a)-(2.10c) restrict values of 6 time-odd coupling constants and leave a freedom to modify the values of  $C_t^s$  and  $C_t^{\Delta s}$ . If one

decides to depart from the complete Skyrme-interaction functional, in which the time-odd coupling constants are uniquely defined by the time-even ones (Appendix A), one may, in principle, use arbitrary values of  $C_t^s$  and  $C_t^{\Delta s}$ . However, independent variations of these coupling constants have never been considered in the literature, and their effects are, up to now, unknown. Therefore, in the present study we restrict our analysis to the functionals in which one or more of the SkM\* coupling constants, Table I, are assumed to be equal to zero. Moreover, in order to further restrict the number of possible variants, we only consider simultaneous modifications of the isoscalar and isovector coupling constants of a given species. In the frame of gauge-invariant functionals, this leaves us a possibility of putting  $C_t^s=0$  and/or  $C_t^{\Delta s}=0$ .

Another modified gauge-invariant functional can be obtained by removing the term  $\mathbf{s}_t \cdot \mathbf{T}_t - \overleftrightarrow{J}_t^2$ , i.e., by putting  $C_t^T = C_t^J = 0$ , in accordance with Eq. (2.10b). This leads to a modification of time-odd *and* time-even mean fields. However, the term  $\overleftrightarrow{J}_t^2$  was anyhow neglected in most parametrizations of the Skyrme forces used for time-even studies, and in particular in SkM\*. Therefore, below we discuss four possibilities corresponding to (i) the complete functional, (ii)  $C_t^T = C_t^J = 0$ , (iii)  $C_t^{\Delta s} = C_t^T = C_t^J = 0$ , and then (iv)  $C_t^s = C_t^{\Delta s} = C_t^T = C_t^J = 0$ . The results are presented in Figs. 3 and 4 for the pairs of bands  $^{151}\text{Tb}(2)$ – $^{152}\text{Dy}(1)$  and  $^{150}\text{Gd}(2)$ – $^{151}\text{Tb}(1)$ , respectively. We have studied several other possibilities, but principal conclusions can be drawn from these four cases.

For  $^{152}\text{Dy}(1)$ , the dynamical moments  $\mathcal{J}^{(2)}$ , Fig. 3(a), are (at high spin) sensitive only to the  $C_t^T = C_t^J$  coupling constants. The influence of  $C_t^{\Delta s}$  and  $C_t^s$  is visible only at low spins, and moreover, their effects have opposite signs and partially cancel one another. Removing from the functional the term  $\mathbf{s}_t \cdot \mathbf{T}_t - \overleftrightarrow{J}_t^2$  decreases the dynamical moments, and, at the high-spin-end of the band, brings the calculated value down to the experimental result. At lower spins one obtains a smaller than previously overestimation of the data (by about 5%).

A very interesting result is obtained for the relative dynamical moments  $\delta\mathcal{J}^{(2)}$ , Fig. 3(b). For any studied combination of the time-odd mean fields taken into account, the dynamical moments in both nuclei are almost identical. Even if the *values* of  $\mathcal{J}^{(2)}$  depend on whether the term  $\mathbf{s}_t \cdot \mathbf{T}_t - \overleftrightarrow{J}_t^2$  is taken into account or not, the *differences* of  $\mathcal{J}^{(2)}$  do not depend on it at all. This is a rather general observation, valid also for other cases of modified functionals discussed below. It means that the identity of dynamical moments is fairly independent of at least some of the details of effective interactions, and can probably be attributed to rather simple geometric effects.

The relative alignments  $\delta I$ , Fig. 3(c), very strongly depend on the presence of the  $\mathbf{s}_t \cdot \mathbf{T}_t - \overleftrightarrow{J}_t^2$  term and are almost independent of the  $\mathbf{s}_t^2$  and  $\mathbf{s}_t \cdot \Delta \mathbf{s}_t$  terms. As soon as  $C_t^T = C_t^J = 0$ , the value of  $\delta I$  at  $\omega = 0.3 \text{ MeV}/\hbar$  comes down to the experimental result. On the other hand, the increase of  $\delta I$  as function of the angular frequency is still too large, and does not give the experimental identity of the  $\gamma$ -transition energies, Eq. (3.1).

In Fig. 4, for the pairs of bands  $^{150}\text{Gd}(2)$ – $^{151}\text{Tb}(1)$  we present a similar analysis of the role of different time-odd terms in the Skyrme functional. In this case, the influence of the  $\mathbf{s}_t \cdot \mathbf{T}_t - \overleftrightarrow{J}_t^2$  term on  $\mathcal{J}^{(2)}$  is weaker than for the  $^{151}\text{Tb}(2)$ – $^{152}\text{Dy}(1)$  pair, while its removal leads to a good agreement with experiment, with only a slightly too slow decrease of  $\mathcal{J}^{(2)}$  as function of the angular velocity. At the same time the relative alignments become much closer to experimental data, but an overestimation by a few tenths of  $\hbar$  persists at all angular frequencies. The influence of the other two time-odd terms considered here,  $\mathbf{s}_t^2$  and  $\mathbf{s}_t \cdot \Delta \mathbf{s}_t$ ,

is much weaker, although a non-negligible influence on relative alignments can be seen.

We conclude this section by noting that the importance of the gauge-invariant time-odd terms for the rotational properties is *not* simply related to the order of the given term. In fact, the zero-order term  $\mathbf{s}_t^2$ , which depends on the density of spin, has a very small influence on the results. At the same time, two second-order terms,  $\mathbf{s}_t \cdot \Delta \mathbf{s}_t$  and  $\mathbf{s}_t \cdot \mathbf{T}_t - \overset{\leftrightarrow}{J}_t^2$ , which in the previous studies have been simultaneously neglected, have a small and rather large influence, respectively. On the other hand, the latter term, which in principle cannot be neglected because of its magnitude, leads to larger deviations from experimental data, as compared with calculations which do disregard it. Of course, the present analysis is not sufficient for a more accurate derivation of the magnitude of coupling constants from experiment. This can only be done by a simultaneous consideration of many different available data, and moreover, should also involve a careful readjustment of properties of the time-even components of the mean fields.

### C. Modified gauge-violating Skyrme functionals

In this Section we present results of calculations for Skyrme functionals with coupling constants which do not obey the gauge-invariance conditions (2.10a)-(2.10c). In order to simplify the discussion, the gauge-invariant time-odd terms  $\mathbf{s}_t^2$  and  $\mathbf{s}_t \cdot \Delta \mathbf{s}_t$  are disregarded, i.e.,  $C_t^s = C_t^{\Delta s} = 0$ . Similarly as in the previous Section, we only consider simultaneous modifications of the isoscalar and isovector coupling constants. This leaves us with a possibility of modifying the time-odd coupling constants,  $C_t^j$ ,  $C_t^T$ , and  $C_t^{\nabla j}$ , while leaving unchanged their time-even gauge-invariance partners,  $C_t^r$ ,  $C_t^J$ , and  $C_t^{\nabla J}$ .

First we have checked the separate role of the time-even and time-odd parts in the term  $\mathbf{s}_t \cdot \mathbf{T}_t - \overset{\leftrightarrow}{J}_t^2$  which has been discussed in the previous Section. It turned out that the time-even part,  $\overset{\leftrightarrow}{J}_t^2$ , influences the results for rotational properties in a negligible way. Therefore, for all practical purposes the results discussed previously should be attributed to the time-odd part,  $\mathbf{s}_t \cdot \mathbf{T}_t$ . This allows us to concentrate here on the two other time-odd terms,  $\mathbf{j}_t^2$  and  $\mathbf{s}_t \cdot (\nabla \times \mathbf{j}_t)$ .

It is worth recalling at this point that in the gauge-invariant energy functional (2.11) the  $\mathbf{j}_t^2$  term is associated with the effective-mass term  $\rho_t \tau_t$ , and the term  $\mathbf{s}_t \cdot (\nabla \times \mathbf{j}_t)$  comes together with the spin-orbit term  $\rho_t (\nabla \cdot \mathbf{J}_t)$ . Therefore, the first one is absent in any theory which has the effective mass  $m^*$  equal to the free mass  $m$ . This is the case for all studies based on phenomenological single-particle potentials, like the Nilsson or WS ones.

On the other hand, the spin-orbit term is crucially important for a correct ordering of single-particle shells and is always taken into account in realistic calculations. However, the studies based on phenomenological potentials always disregard its time-odd gauge partner, and therefore should be considered as gauge-violating approaches, similar to the selfconsistent calculations considered in this Section.

In Figs. 5 and 6 we present the results obtained for the same pairs of superdeformed bands as considered above, namely, for  $^{151}\text{Tb}(2) - ^{152}\text{Dy}(1)$  and  $^{150}\text{Gd}(2) - ^{151}\text{Tb}(1)$ , respectively. Open symbols refer to the functionals with  $C_t^j = 0$  and squares to those with  $C_t^{\nabla j} = 0$ . Consequently, the full circles repeat here the same results as those shown by full circles in Figs. 3 and 4. On the other hand, open squares correspond to the Skyrme functionals with

all time-odd terms neglected.

As expected from the semiclassical analysis [43], omitting the  $\mathbf{j}_t^2$  term leads to much smaller values of  $\mathcal{J}^{(2)}$ . The obtained decrease is of the order of 10-13%, depending on the value of the angular frequency, i.e., it is much smaller than the decrease of about 40% obtained from non-selfconsistent estimates [43]. With a very high precision, this decrease is identical for both nuclei in pairs differing by a hole in the  $\pi[301]1/2$  ( $r=+i$ ) orbital. Indeed, even if the values of  $\mathcal{J}^{(2)}$  change by as much as  $13\hbar^2\text{MeV}^{-1}$ , the relative dynamical moments, Figs. 5(b) and 6(b), do not change at all, and are always well below  $1\hbar^2\text{MeV}^{-1}$ . In addition, the  $\mathbf{j}_t^2$  term has only a minor influence on the values of relative alignments  $\delta I$ .

The presence of the second term studied here,  $\mathbf{s}_t \cdot (\nabla \times \mathbf{j}_t)$ , has very little effect on the values and relative values of  $\mathcal{J}^{(2)}$ . However, its impact on the values of relative alignments is very large. Removing this term from the functional, decreases the values of  $\delta I$  by about  $0.5\hbar$ . For the  $^{151}\text{Tb}(2)$ - $^{152}\text{Dy}(1)$  pair of bands, this leads to relative alignment which has the experimental value at the high-spin end of the band, Fig. 5(c). At the low-spin end the value of  $\delta I$  is now underestimated by about  $0.3\hbar$ . According to Eq. (3.1), this gives the differences of the  $\gamma$ -ray energies increasing from about  $-6\text{keV}$  to 0, i.e., the identity of  $E_\gamma$  is still not reproduced with a sufficient precision. The sensitivity of results to the  $C_t^{\nabla j}$  coupling constant suggests, however, that a fit of this kind of term to experimental data may, in principle, improve the agreement. As mentioned previously, such a fit should take into account many different bands and cannot be based on a rather restricted set of examples discussed here.

For the  $^{150}\text{Gd}(2)$ - $^{151}\text{Tb}(1)$  pair of bands, the removal of the  $\mathbf{s}_t \cdot (\nabla \times \mathbf{j}_t)$  term, while keeping the term  $\mathbf{j}_t^2$  unchanged, leads to a very good description of the values of  $\mathcal{J}^{(2)}$ , and of the relative alignments  $\delta I$  simultaneously, Fig. 6. In this case, the relative alignments agree with the experiment to better than  $0.1\hbar$ , which corresponds to the identity of the  $\gamma$ -ray energies to better than  $1\text{keV}$ .

#### IV. CONCLUSIONS

In the present study we have applied the Hartree-Fock cranking method with the Skyrme interactions to describe rotational states in selected superdeformed nuclei. We have analyzed in detail properties of two pairs of bands, namely,  $^{151}\text{Tb}(2)$ - $^{152}\text{Dy}(1)$  and  $^{150}\text{Gd}(2)$ - $^{151}\text{Tb}(1)$ . Experimentally, these bands are pair-wise identical, i.e., the corresponding  $\gamma$ -transition energies are identical within  $2\text{keV}$  each.

In agreement with the previous interpretations, we have fixed the configurations of the  $^{151}\text{Tb}(1)$  band as a hole-structure created in the  $\pi[651]3/2$  ( $r=+i$ ) or  $\pi 6_4$  Nilsson intruder orbital with respect to the magic superdeformed  $^{152}_{66}\text{Dy}_{86}$  core. Similarly, the  $^{151}\text{Tb}(2)$  and  $^{150}\text{Gd}(2)$  bands have been constructed as the  $\pi[301]1/2$  ( $r=+i$ ) hole configurations in the corresponding  $^{152}\text{Dy}(1)$  and  $^{151}\text{Tb}(1)$  cores.

The dynamical moments  $\mathcal{J}^{(2)}$  calculated for the  $^{151}\text{Tb}(2)$ - $^{152}\text{Dy}(1)$  pair of bands and for the  $^{150}\text{Gd}(2)$ - $^{151}\text{Tb}(1)$  pair of bands are identical within  $2\hbar^2\text{MeV}^{-1}$ . This result correctly reproduces the identity of these two pairs of bands obtained in experiment. It confirms that the internal structure of the  $\pi[301]1/2$  ( $r=+i$ ) orbital is responsible for the occurrence of these particular identical bands. The obtained identity of  $\mathcal{J}^{(2)}$  does not depend on the version of the Skyrme force used, neither it depends on including or disregarding various

time-odd components in the mean field of the rotating nucleus. The fact that the two bands calculated in  $^{151}\text{Tb}$ , i.e.,  $^{151}\text{Tb}(1)$  and  $^{151}\text{Tb}(2)$ , are *not* identical (similarly as in experiment), indicates a crucial role of the single-particle structure of the involved orbitals, and shows that in the HF cranking theory the phenomenon of identical bands is not a generic, built-in-by-assumption result.

The relative alignments of the studied pairs of bands are more difficult to reproduce than the simple identity of the dynamical moments. First of all, the results do depend on the version of Skyrme interaction and on the time-odd components included in the mean field. When the complete Skyrme functionals are used, i.e., when all time-odd terms are taken into account, the calculated relative alignments do not reproduce the experimental data. The disagreement obtained for the SkM\* interaction is particularly large, while the SIII and SkP interactions also give too large relative alignments. Within the SkM\* parametrization, good agreement with data is obtained when all time-odd terms are disregarded except of the one which involves the density of current,  $\mathbf{j}$ , and is related to the effective-mass term by the gauge transformation.

This specific result does not imply that the time-odd terms present in the formalism should be generally eliminated from its applications. By studying cases with some time-odd terms removed we only aimed at gaining information which may be useful when improving the parametrisation of effective interactions.

As seen from the results obtained in the present study, a readjustment of parameters of effective forces in the time-odd channel seems to be necessary for a detailed description of the identical  $\gamma$ -ray transitions in superdeformed nuclei. However, this should be done by taking into account many available high-spin data simultaneously, and also should involve a readjustment of the time-even part (the spin-orbit interaction, in particular) which is responsible for the ordering of the single-particle energies and routhians. The work along these lines is now in progress.

## ACKNOWLEDGMENTS

We would like to express our thanks to the *Institut du Développement et de Ressources en Informatique Scientifique* (IDRIS) of CNRS, France, which provided us with the computing facilities under Project no. 940333. This research was supported in part by the Polish Committee for Scientific Research under Contract No. 2 P03B 034 08.

## APPENDIX A: COUPLING CONSTANTS OF THE SKYRME FUNCTIONAL

In its standard form, the Skyrme interaction (see e.g. Ref. [12]) depends on 10 parameters,  $t_0$ ,  $x_0$ ,  $t_1$ ,  $x_1$ ,  $t_2$ ,  $x_2$ ,  $t_3$ ,  $x_3$ ,  $\alpha$ , and  $W$ . For  $x_1=x_2=0$ , the energy density which corresponds to the Skyrme interaction has been derived in Ref. [26]. In terms of the isovector and isoscalar coupling constants, and for the complete interaction, this energy density is given in Eqs. (2.2)–(2.4).

The zero-order coupling constants,  $C_t^p$  and  $C_t^s$ , correspond to the velocity-independent terms of the interaction, and can be expressed by the  $t_0$ ,  $x_0$ ,  $t_3$ , and  $x_3$  parameters, as it

shows Table III. The zero-order time-odd coupling constants  $C_t^s$  (for  $t=0$  and 1) are linear combinations of the zero-order time-even coupling constants  $C_t^\rho$  (Table IV).

Similarly, the second-order coupling constants,  $C_t^{\Delta\rho}$ ,  $C_t^\tau$ ,  $C_t^{\Delta s}$ , and  $C_t^T$ , correspond to the velocity-dependent terms of the interaction given by the parameters  $t_1$ ,  $x_1$ ,  $t_2$ , and  $x_2$ , and are presented in Table V. The second-order time-odd coupling constants,  $C_t^{\Delta s}$  and  $C_t^T$ , are linear combinations of the second-order time-even coupling constants,  $C_t^{\Delta\rho}$  and  $C_t^\tau$  (Table VI). Another four second-order coupling constants,  $C_t^J$  and  $C_t^j$ , which also depend on the same  $t_1$ ,  $x_1$ ,  $t_2$ , and  $x_2$  parameters, are given by the gauge-invariance conditions (2.10a) and (2.10b).

Finally, the second-order coupling constants  $C_t^{\nabla J}$  are given by the spin-orbit term of the Skyrme interaction and depend on the parameter  $W$ ,  $C_0^{\nabla J} = -\frac{3}{4}W$  and  $C_1^{\nabla J} = -\frac{1}{4}W$ , while the other two,  $C_t^{\nabla j}$ , follow from the gauge-invariance condition (2.10c). An extension of the Skyrme energy density, which introduces the coupling constants  $C_0^{\nabla J}$  and  $C_1^{\nabla J}$  independent of one another, is discussed in Ref. [44]

## REFERENCES

- [1] P. Ring and P. Schuck, *The Nuclear Many-Body Problem* (Springer, Berlin, 1980).
- [2] S. Åberg, H. Flocard and W. Nazarewicz, *Ann. Rev. Nucl. Part. Sci.* **40**, 439 (1990); and references therein.
- [3] M. Baranger and M. Vénéroni, *Ann. of Phys.* **114**, 123 (1978).
- [4] B. Grammaticos and A. Voros, *Ann. of Phys.* **123**, 359 (1979); **129**, 153 (1980).
- [5] D.J. Thouless and J.G. Valatin, *Nucl. Phys.* **A31**, 211 (1962).
- [6] A. Bohr and B.R. Mottelson, *Nuclear Structure*, vol. 2 (W.A. Benjamin, New York, 1975).
- [7] A.B. Migdal, *Nucl. Phys.* **13**, 655 (1959).
- [8] M.J. Giannoni and P. Quentin, *Phys. Rev.* **C21**, 2076 (1980).
- [9] J. Dobaczewski and J. Skalski, *Nucl. Phys.* **A369**, 123 (1981).
- [10] Z. Szymański, *Fast nuclear rotation* (Clerandon, Oxford, 1983).
- [11] K. Neergård, V.V. Pashkevich, and S. Frauendorf, *Nucl. Phys.* **A262**, 61 (1976).
- [12] P. Bonche, H. Flocard and P.-H. Heenen, *Nucl. Phys.* **A467**, 115 (1987).
- [13] P. Bonche, H. Flocard and P.-H. Heenen, *Nucl. Phys.* **A523**, 300 (1991).
- [14] B.Q. Chen, P.-H. Heenen, P. Bonche, M.S. Weiss and H. Flocard, *Phys. Rev.* **C46**, 1582 (1992).
- [15] B. Gall, P. Bonche, J. Dobaczewski, H. Flocard, and P.-H. Heenen, *Z. Phys.* **A348**, 183 (1994).
- [16] H. Flocard, P. Bonche, P.-H. Heenen, and R. Mehrem, *Proceedings of the Antibes Conference*, 1994.
- [17] J. Terasaki, P.-H. Heenen, P. Bonche, J. Dobaczewski, and H. Flocard, to be published.
- [18] P.-H. Heenen, P. Bonche, and H. Flocard, submitted to *Nucl. Phys.*
- [19] P. Bonche, H. Flocard, and P.-H. Heenen, to be published.
- [20] W. Koepf and P. Ring, *Nucl. Phys.* **A493**, 61 (1989); **A511**, 279 (1990).
- [21] J. König and P. Ring, *Phys. Rev. Lett.* **71**, 3079 (1993).
- [22] J.L. Egido and L.M. Robledo, *Phys. Rev. Lett.* **70**, 2876 (1993).
- [23] R.V.F. Janssens and T.L. Khoo, *Ann. Rev. Nucl. Part. Sci.* **41**, 321 (1991); and references therein.
- [24] C. Baktash, B. Haas, and W. Nazarewicz, to be published in *Ann. Rev. Nucl. Part. Sci.*; and references therein.
- [25] D. Vautherin and D.M. Brink, *Phys. Rev.* **C5**, 626 (1972).
- [26] Y.M. Engel, D.M. Brink, K. Goeke, S.J. Krieger, and D. Vautherin, *Nucl. Phys.* **A249**, 215 (1975).
- [27] S. Krewald, V. Klemt, J. Speth, and A. Faessler, *Nucl. Phys.* **A281**, 166 (1977).
- [28] C.J. Pethick, D.G. Ravenhall, and C.P. Lorentz, Urbana preprint P-94-08-068.
- [29] M. Beiner, H. Flocard, N. Van Giai and P. Quentin, *Nucl. Phys.* **A238**, 29 (1975).
- [30] J.W. Negele and D. Vautherin, *Phys. Rev.* **C5**, 1472 (1972).
- [31] J. Dobaczewski and J. Dudek, to be submitted to *Computer Physics Communications*.
- [32] J. Dudek, Z. Szymański, and T.R. Werner, *Phys. Rev.* **C23**, 920 (1981).
- [33] S. Ówiok, J. Dudek, W. Nazarewicz, J. Skalski, and T. Werner, *Comp. Phys. Commun.* **46**, 379 (1987).
- [34] J. Bartel, P. Quentin, M. Brack, C. Guet, and H.B. Håkansson, *Nucl. Phys.* **A386**, 79 (1982).

- [35] J. Dobaczewski, H. Flocard, and J. Treiner, Nucl. Phys. **A422**, 103 (1984).
- [36] J. Dobaczewski, W. Nazarewicz, and T.R. Werner, Physica Scripta, in press.
- [37] C.W. Beausang *et al.*, Phys. Rev. Lett. **71**, 1800 (1993).
- [38] P.J. Dagnall *et al.*, Phys. Lett. **B335**, 313 (1994).
- [39] B. Kharraja *et al.*, Phys. Lett. **B341**, 268 (1995).
- [40] Th. Byrski *et al.*, Phys. Rev. Lett. **64**, 1650 (1990).
- [41] W. Nazarewicz, P.J. Twin, P. Fallon, and J.D. Garrett, Phys. Rev. Lett. **64**, 1654 (1990).
- [42] I. Ragnarsson, Nucl. Phys. **A557**, 167c (1993).
- [43] K. Bencheikh, P. Quentin, and J. Bartel, Nucl. Phys. **A571**, 518 (1994).
- [44] P.-G. Reinhard and H. Flocard, Orsay preprint 1994.

TABLES

TABLE I. Coupling constants in the gauge-invariant energy density (2.11) obtained for the SIII, SkP, and SkM\* Skyrme interactions. Zero-order coupling constants  $C_t^\rho$  and  $C_t^s$  are given in  $\text{MeV}\cdot\text{fm}^3$  and the remaining (second-order) ones are given in  $\text{MeV}\cdot\text{fm}^5$ .

	$t=0$			$t=1$		
	SIII	SkM*	SkP	SIII	SkM*	SkP
$C_t^\rho(\rho=0)$	-423.3	-991.9	-1099.4	268.8	390.1	580.6
$C_t^\rho(\rho=\rho_{\text{nm}})$	-296.4	-237.7	-335.6	141.2	150.8	188.4
$C_t^{\Delta\rho}$	-63.0	-68.2	-60.1	17.0	17.1	35.1
$C_t^\tau$	44.4	34.7	0.0	-30.6	-34.1	-44.6
$C_t^{\nabla J}$	-90.0	-97.5	-75.0	-30.0	-32.5	-25.0
$C_t^s(\rho=0)$	14.1	271.1	152.3	141.1	330.6	366.5
$C_t^s(\rho=\rho_{\text{nm}})$	56.4	31.7	-31.4	98.8	91.2	78.5
$C_t^{\Delta s}$	17.0	17.1	-4.2	17.0	17.1	9.8
$C_t^T$	-30.6	-34.1	7.7	-30.6	-34.1	-41.1

TABLE II. Proton quadrupole moments (in barns) calculated for the SIII, SkM\*, and SkP Skyrme forces at  $\omega=0.5\text{ MeV}/\hbar$ .

	SIII	SkM*	SkP
$^{152}\text{Dy}(1)$	18.55	18.25	18.36
$^{151}\text{Tb}(2)$	18.69	18.38	18.48
$^{151}\text{Tb}(1)$	17.59	17.22	17.41
$^{150}\text{Gd}(2)$	17.74	17.36	17.54

TABLE III. Zero-order coupling constants as functions of parameters of the Skyrme interactions, expressed by the formula:  $C = \frac{1}{8}(at_0 + bt_0x_0) + \frac{1}{48}\rho^\alpha(at_3 + bt_3x_3)$ .

	$a$	$b$
$C_0^\rho$	3	0
$C_1^\rho$	-1	-2
$C_0^s$	-1	2
$C_1^s$	-1	0

TABLE IV. Zero-order time-odd coupling constants as functions of the time-even coupling constants, expressed by the formula:  $C = \frac{1}{3}(aC_0^\rho + bC_1^\rho)$ .

	$a$	$b$
$C_0^s$	-2	-3
$C_1^s$	-1	0

TABLE V. Second-order coupling constants as functions of parameters of the Skyrme interactions, expressed by the formula:  $C = \frac{1}{64}(at_1 + bt_1x_1 + ct_2 + dt_2x_2)$ .

	$a$	$b$	$c$	$d$
$C_0^{\Delta\rho}$	-9	0	5	4
$C_1^{\Delta\rho}$	3	6	1	2
$C_0^T$	12	0	20	16
$C_1^T$	-4	-8	4	8
$C_0^{\Delta s}$	3	-6	1	2
$C_1^{\Delta s}$	3	0	1	0
$C_0^T$	-4	8	4	8
$C_1^T$	-4	0	4	0

TABLE VI. Second-order time-odd coupling constants as functions of the time-even coupling constants, expressed by the formula:  $C = \frac{1}{24}(aC_0^{\Delta\rho} + bC_1^{\Delta\rho} + cC_0^T + dC_1^T)$ .

	$a$	$b$	$c$	$d$
$C_0^{\Delta s}$	0	6	3	9
$C_1^{\Delta s}$	-4	-4	3	-3
$C_0^T$	0	48	-4	12
$C_1^T$	16	-16	4	-12

## FIGURES

FIG. 1. Calculated dynamical moment  $\mathcal{J}^{(2)}$  for the yrast band of  $^{152}\text{Dy}$ , part (a), the relative dynamical moment  $\delta\mathcal{J}^{(2)}$  calculated for the  $^{151}\text{Tb}(2)$  and  $^{152}\text{Dy}(1)$  bands, part (b), and the relative alignment  $\delta I$  between these two bands, part (c). The experimental points are denoted by asterisks. Complete Skyrme functionals of SIII, SkM\*, and SkP interactions have been used. Note the scale in (b) expanded five times as compared to (a).

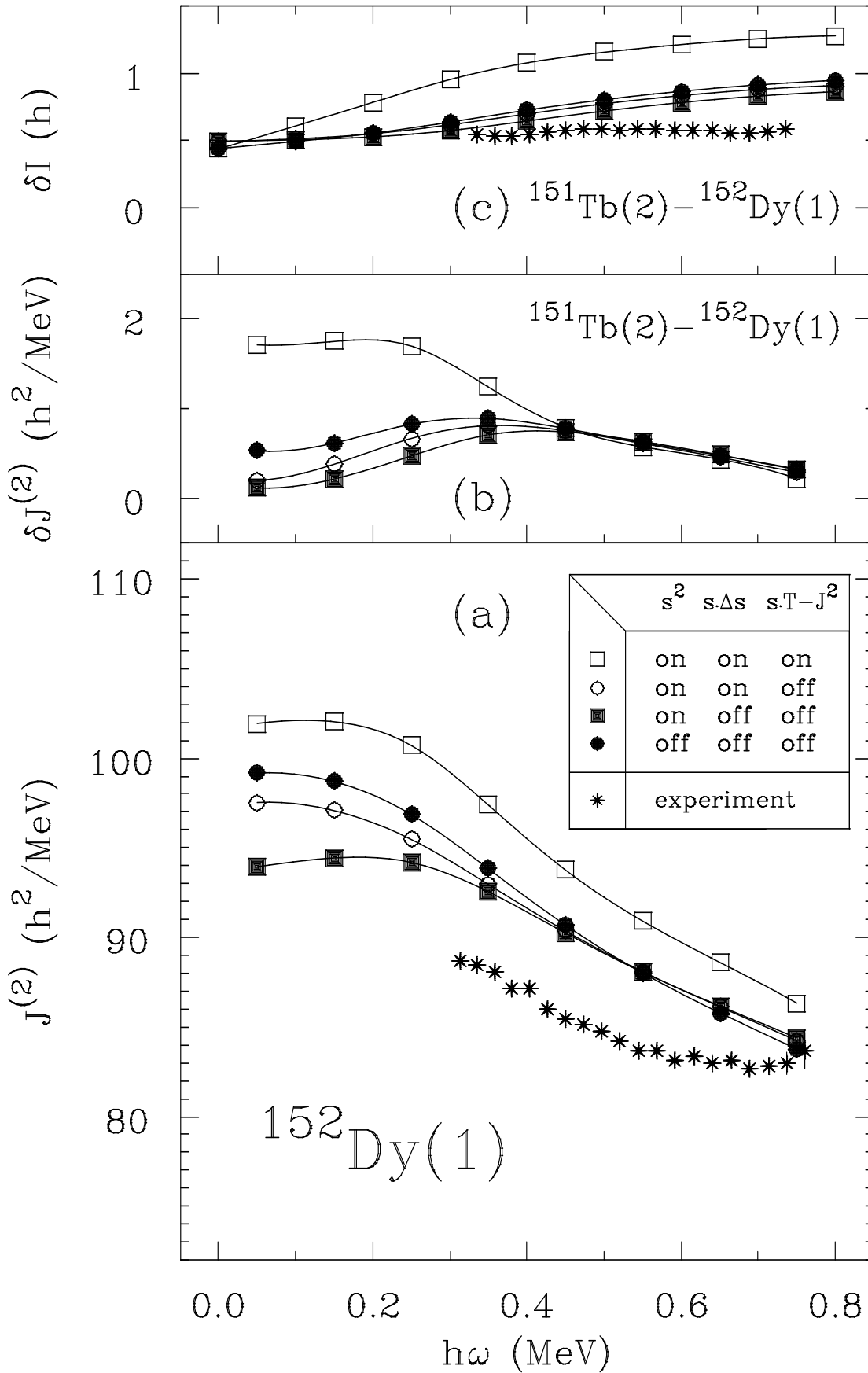
FIG. 2. Same as Fig. 1, but for the  $^{151}\text{Tb}(1)$  band, (a), and for the differences between the  $^{150}\text{Gd}(2)$  and  $^{151}\text{Tb}(1)$  bands, (b) and (c).

FIG. 3. Same as Fig. 1, but for the complete SkM\* functional (open squares) compared to three versions of the modified SkM\* functional, namely,  $C_t^T=0$  (open circles),  $C_t^T=C_t^{\Delta s}=0$  (full squares), and  $C_t^T=C_t^{\Delta s}=C_t^s=0$  (full circles). The modified functionals are gauge invariant, i.e.,  $C_t^J=0$  whenever  $C_t^T=0$ , Eq.(2.10b).

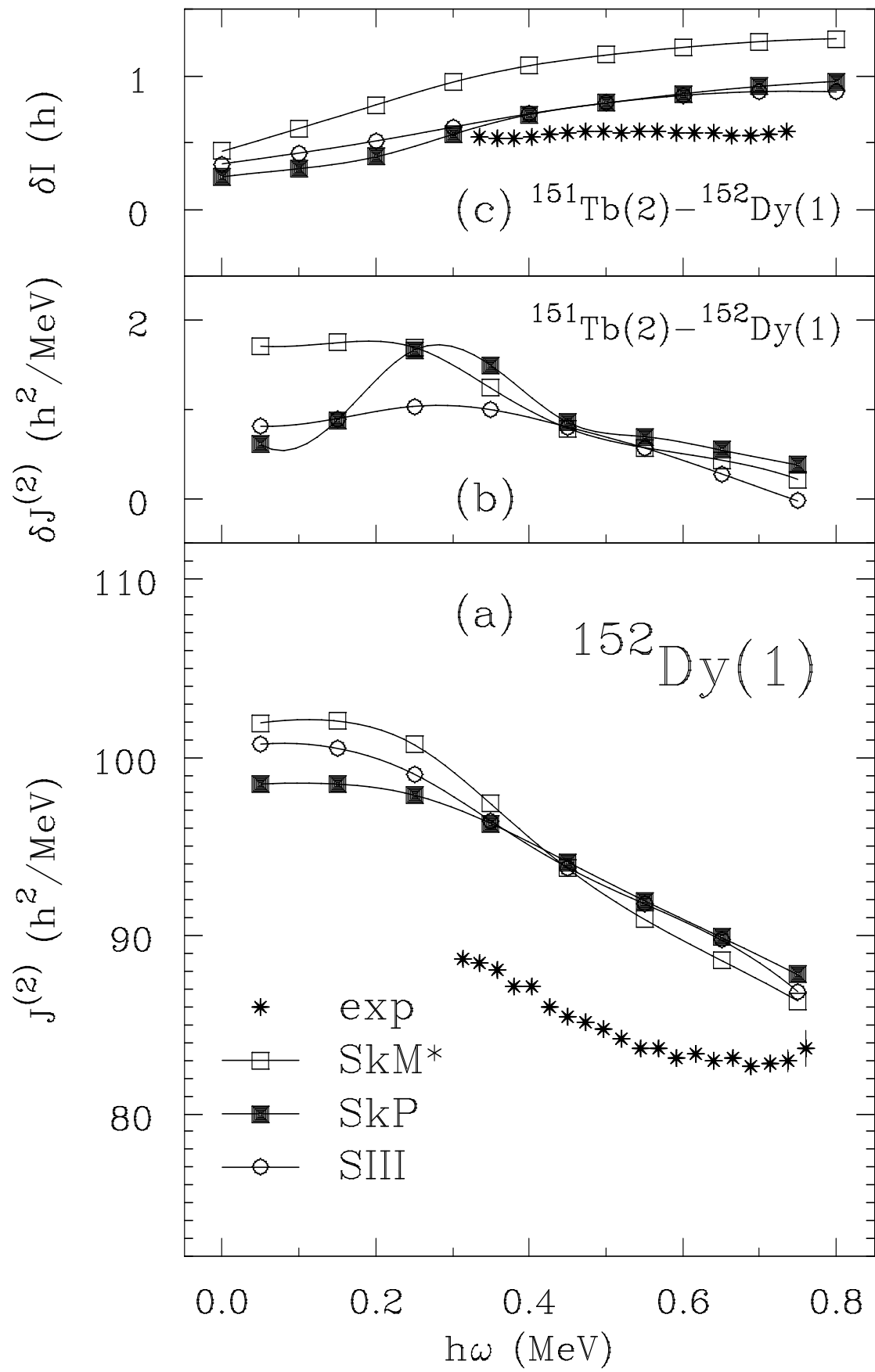
FIG. 4. Same as Fig. 3, but for the  $^{150}\text{Gd}(2)$ - $^{151}\text{Tb}(1)$  pair of bands.

FIG. 5. Same as Fig. 3, but for the modified gauge-invariant SkM\* functional given by  $C_t^T=C_t^{\Delta s}=C_t^s=0$  (full circles), compared to three versions of the gauge-violating SkM\* functional obtained by putting in addition  $C_t^j=0$  (open symbols) and/or  $C_t^{\nabla j}=0$  (squares). The version with  $C_t^j=C_t^{\nabla j}=0$  (open squares) corresponds to all mean-field time-odd terms neglected.

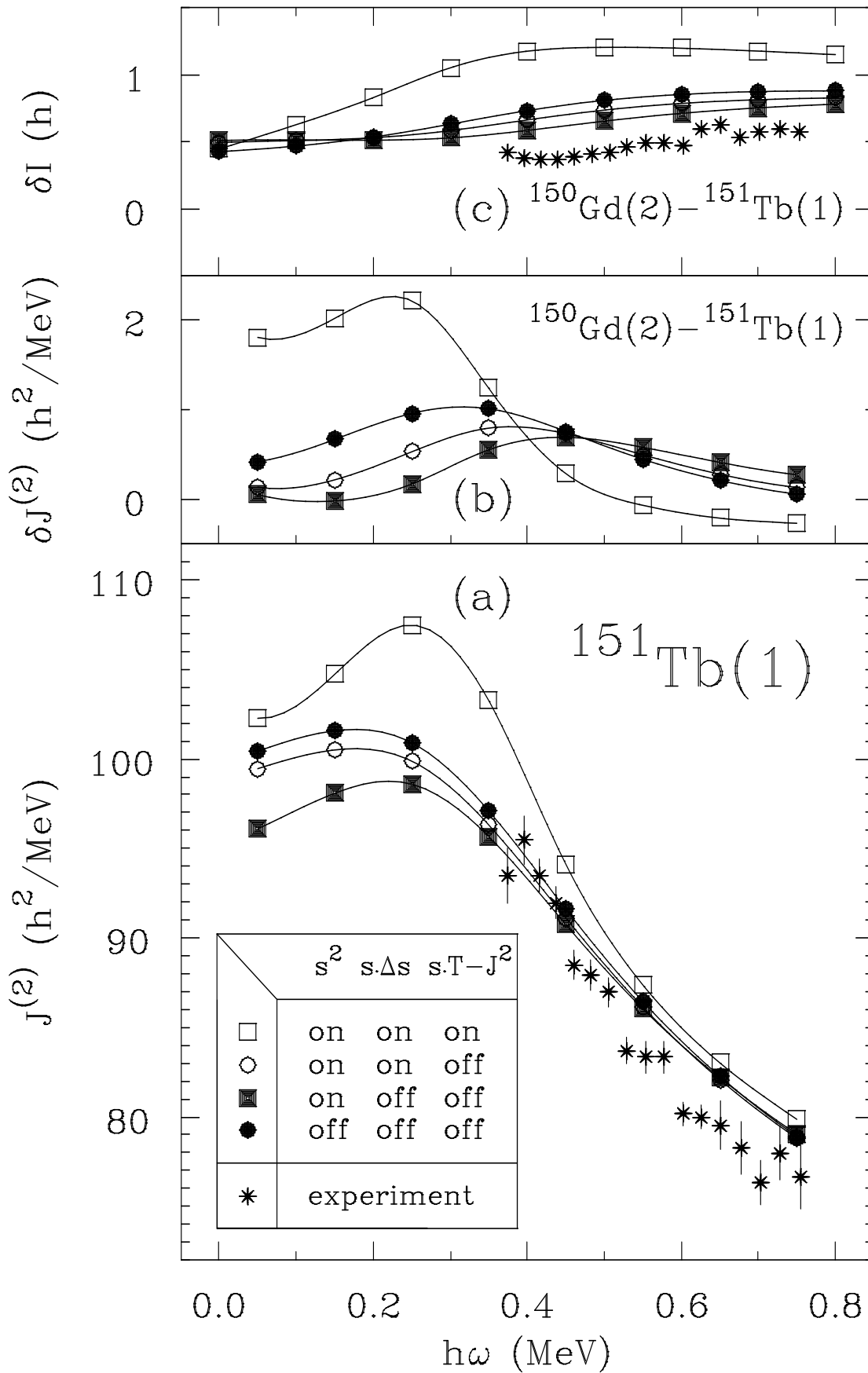
FIG. 6. Same as Fig. 5, but for the  $^{150}\text{Gd}(2)$ - $^{151}\text{Tb}(1)$  pair of bands.



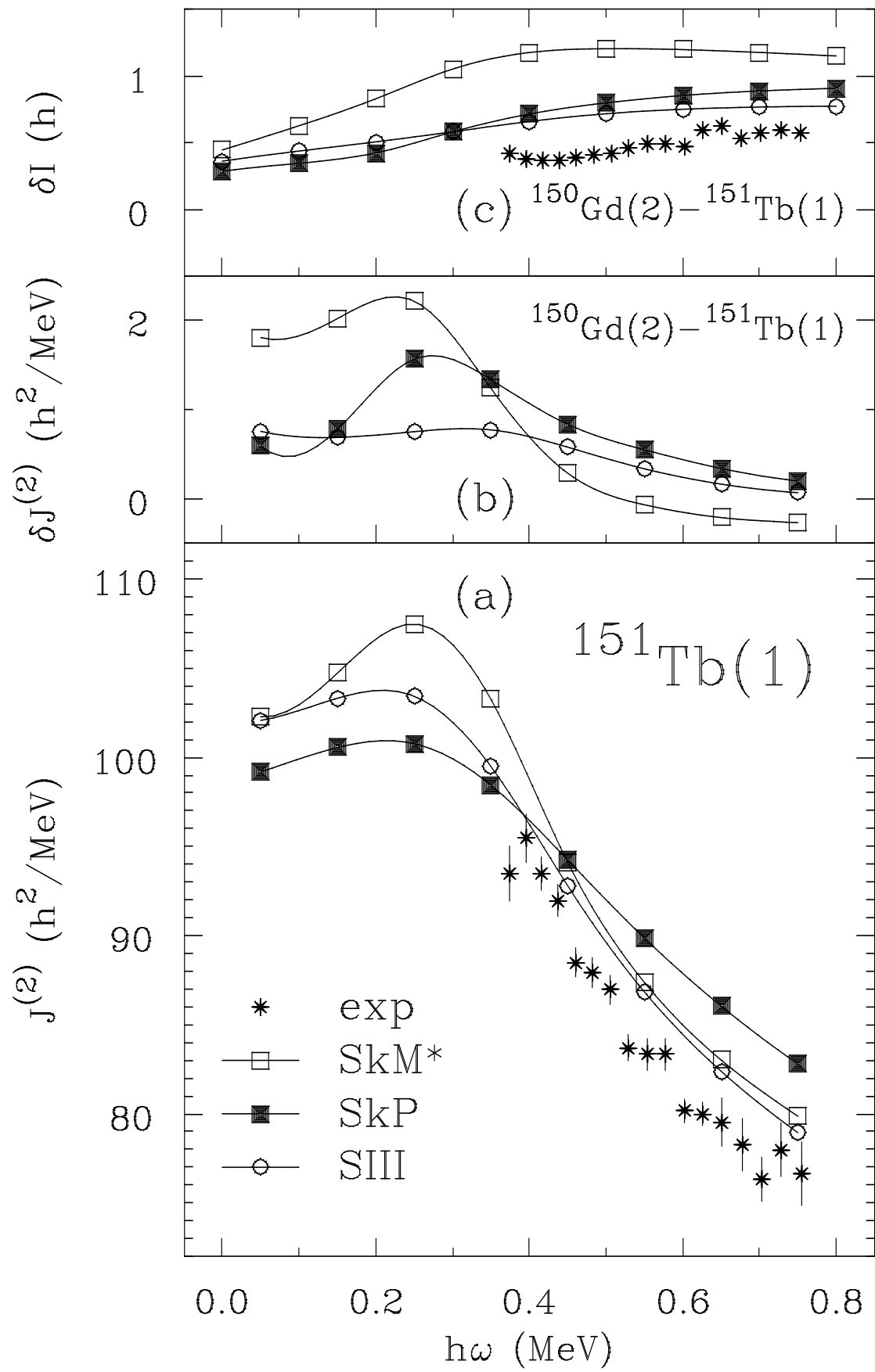
Cranked Hartree-Fock

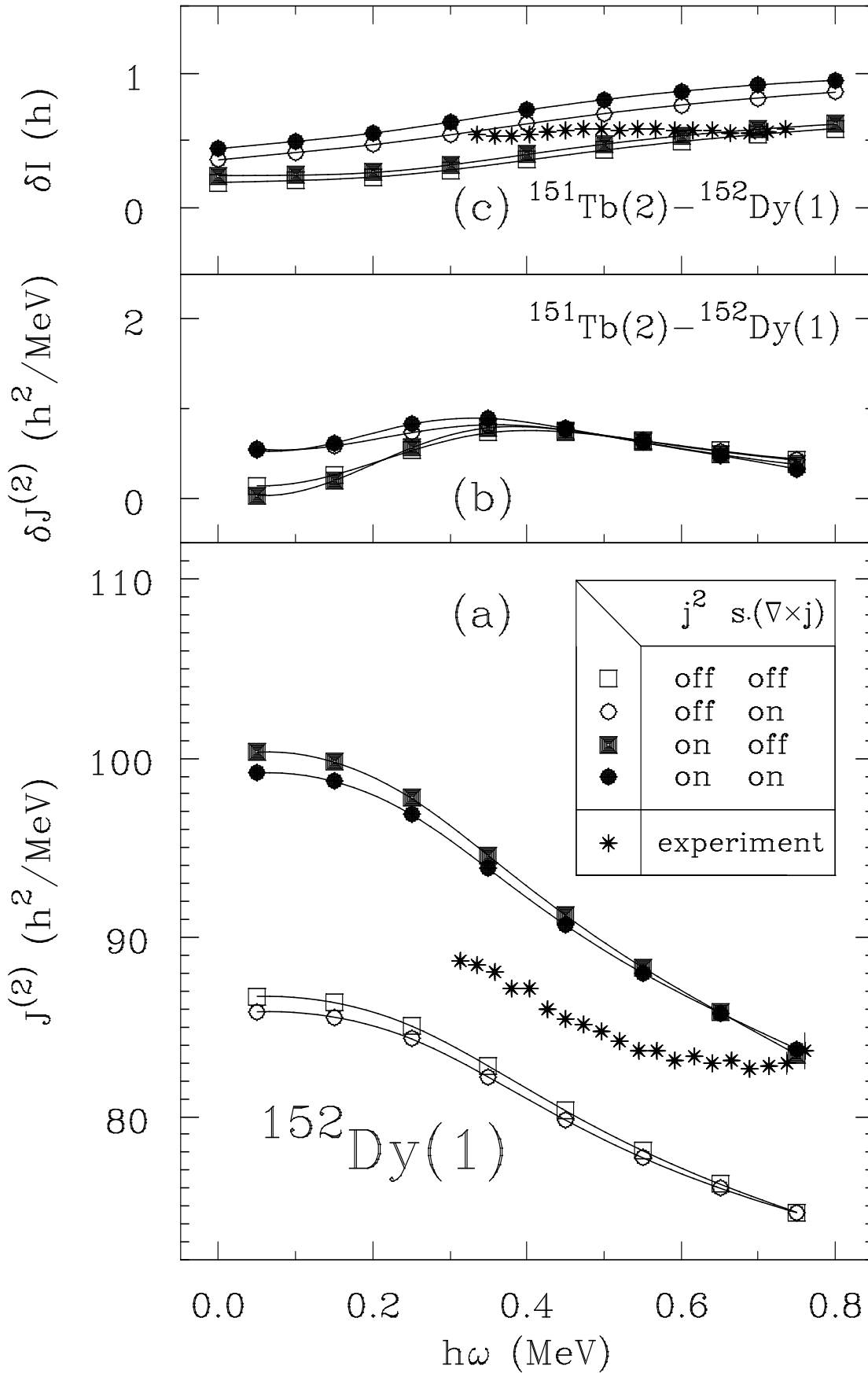


Cranked Hartree-Fock - Skyrme SkM\*



Cranked Hartree-Fock





Cranked Hartree-Fock - Skyrme SkM\*

